


## Article

# Characteristics of Atmospheric Ice Nucleation during Spring: A Case Study on Huangshan

Kui Chen <sup>1</sup>, Xinhan Chen <sup>1</sup>, Shichao Zhu <sup>2</sup>, Lei Ji <sup>2</sup> and Yan Yin <sup>3,\*</sup>

<sup>1</sup> School of Emergency Management, Nanjing University of Information Science and Technology, Nanjing 210044, China; 001489@nuist.edu.cn (K.C.); 202212480008@nuist.edu.cn (X.C.)

<sup>2</sup> Anhui Artificial Weather Modification Office, Hefei 210031, China; zsc-6387099@163.com (S.Z.); clubbin@126.com (L.J.)

<sup>3</sup> Key Laboratory for Aerosol-Cloud-Precipitation of China Meteorological Administration, Nanjing University of Information Science and Technology, Nanjing 210044, China

\* Correspondence: yinyan@nuist.edu.cn; Tel.: +86-25-5873-1207

**Abstract:** Atmospheric ice nucleation particles (INPs) play a crucial role in influencing cloud formation and microphysical properties, which in turn impact precipitation and Earth's radiation budget. However, the influence of anthropogenic activities on the properties and concentrations of INPs remains an area of significant uncertainty. This study investigated the physical and chemical characteristics of atmospheric ice nucleation particles in Huangshan, China during the May Day labor holiday period (spanning 8 days, from April 27th to May 5th). INP concentrations were measured at temperatures from  $-17\text{ }^{\circ}\text{C}$  to  $-26\text{ }^{\circ}\text{C}$  and relative humidities ( $\text{RH}_w$ ) from 95% to 101%. Average INP concentrations reached  $13.7\text{ L}^{-1}$  at  $-26\text{ }^{\circ}\text{C}$  and 101% RH, 137 times higher than at  $-17\text{ }^{\circ}\text{C}$  and 95% RH. INP concentrations showed exponential increases with decreasing temperature and exponential increases with increasing RH. Concentration fluctuations were observed over time, with a peak of  $\sim 30\text{ L}^{-1}$  ( $t = -26\text{ }^{\circ}\text{C}$ ,  $\text{RH}_w = 101\%$ ) around the start and end of the holiday period. Aerosol number concentrations were monitored simultaneously. The peak in aerosols larger than  $0.5\text{ }\mu\text{m}$  aligned with the peak in INP concentrations, suggesting a link between aerosol levels and INPs. Chemical composition analysis using SEM-EDX revealed the distinct elemental makeup of INPs based on the activation temperature. INPs active at warmer temperatures contained N, Na, and Cl, indicating possible biomass and sea salt origins, while those active at colder temperatures contained crustal elements like Al and Ca.

**Keywords:** ice nucleation particles; aerosol; chemical elements; numeric concentration; ice nucleation



**Citation:** Chen, K.; Chen, X.; Zhu, S.; Ji, L.; Yin, Y. Characteristics of Atmospheric Ice Nucleation during Spring: A Case Study on Huangshan. *Atmosphere* **2024**, *15*, 629. <https://doi.org/10.3390/atmos15060629>

Academic Editor: Filomena Romano

Received: 10 April 2024

Revised: 20 May 2024

Accepted: 22 May 2024

Published: 24 May 2024



**Copyright:** © 2024 by the authors. Licensee MDPI, Basel, Switzerland. This article is an open access article distributed under the terms and conditions of the Creative Commons Attribution (CC BY) license (<https://creativecommons.org/licenses/by/4.0/>).

## 1. Introduction

Aerosols serve as the nuclei upon which cloud droplets form [1]. Clouds have a significant impact on Earth's radiation budget [2,3]. Human activity has led to a worldwide rise in the levels of aerosol particles, as well as alterations in cloud condensation nuclei (CCN) and INPs [1,4,5]. The influence of aerosol-induced changes on cloud optical properties and the resulting radiative forcing is the least understood component in the historical radiative forcing of Earth's climate caused by greenhouse gases and aerosols [6,7]. The occurrence of ice nucleation has the capacity to influence the formation of precipitation, the duration of clouds, and the radiative properties of the atmosphere [8–10]. Temperature and ice supersaturation ( $S_{si}$ ) are the primary factors that determine ice nucleation [11,12]. Heterogeneous nucleation occurs at lower levels of supersaturation and higher temperatures than homogeneous nucleation [13,14]. Heterogeneous ice nucleation plays an important role in mixed-phase clouds since it affects the allocation of water between the ice and liquid phases [15,16]. Furthermore, it establishes the duration, radiative impact, and precipitation of clouds [17].

Based on satellite observations and model simulations, it has been determined that INPs play a crucial role in influencing the phase of clouds [18]. INPs have the potential to mix, adsorb, coagulate, or undergo chemical reactions with other substances (such as biological materials, anthropogenic emissions, and secondary products) due to human actions [19,20]. These coatings or reactive substances may alter the ability of INPs to initiate ice formation, thus impacting the creation of clouds and their microphysical properties [21,22]. This adds complexity to the estimation of the influence of aerosols on clouds [23–25]. Increasing knowledge about the characteristics of INPs will improve the accuracy of evaluating the impact of aerosols on clouds and reduce the level of uncertainty involved [18,26].

Several previous ice nucleation studies have been carried out in controlled laboratory settings, providing useful insights into the INP characteristics of individual particles made up of pure components and artificially produced aerosol mixtures [27,28]. Mineral dust and biological particles are generally recognized as potential INPs [29–31]. Nevertheless, the occurrence of ice formation in mixed-phase clouds that contain both soot and organic particles has not been definitively proven due to the varied chemical composition and distinct experimental settings involved [32,33]. Sea salt and sulfates are usually regarded as ineffective INPs in mixed-phase settings [34,35]. However, the situation becomes more intricate in the surrounding atmosphere, where particles often exist as intricate combinations of diverse chemicals and minerals [36,37]. Although recent laboratory experiments have examined the impact of different states of aerosol mixtures [38–40], the atmosphere's complexity has not been accurately simulated. Human activity has caused changes in the physical and chemical characteristics of aerosols, leading to an alteration in the properties of INPs [22,41].

Located in the eastern part of China, Huangshan is a famous tourist destination known for its beautiful scenery and unique weather phenomena. During the eight-day Labor Day holiday, from April 27th to May 5th, there was a substantial surge in the influx of tourists to Huangshan. The influx of tourists led to a rise in emissions from transportation, restaurants/businesses serving visitors, and other human-caused sources. This increase in emissions has the potential to affect the concentration and composition of atmospheric aerosols. Moreover, the rise in the concentration of air particles alters the mechanisms of ice nucleation. The occurrence of tourists influencing the concentration of ice nuclei has also been observed on Mount Tai, as previously reported [42].

The main aim of this work was to clarify the physical and chemical properties of atmospheric INPs and how they may be influenced by human activities. The study involved the collection of INP samples from Huangshan during the observation period. The levels of ice-nucleating particles in deposition mode were quantified using a stationary diffusion cloud chamber. The dimensions and chemical makeup of INPs were ascertained using a scanning electron microscope. The main aim of this study is to investigate the correlation between INP activity and chemical compositions. Furthermore, it provides initial proof that human activities have an impact on the functioning of INPs.

## 2. Materials and Methods

### 2.1. Measurement Site

The field campaign of the weather modification experiment in central China (WMECC) involved measuring the atmospheric characteristics in Huangshan. Figure 1a displays the locations of three field observation points of the WMECC: Guangmingding (30.13° N, 118.16° E, 1840 m above mean sea level (a. m. s. l.)), Yungu Temple (30.10° N, 118.18° E, 890 m a. m. s. l.), and The Anhui Provincial Base for Weather Modification Demonstration at Tangkou (AWMDB, 30.06° N, 118.18° E, 450 m a. m. s. l.). The data collection and analysis in this study were conducted at the AWMDDB during the Labor Day holiday period, specifically from April 27th to May 5th. As shown in Figure 1c,d, a series of meteorological and atmospheric composition instruments of the AWMDDB were deployed to measure key meteorological, pollution gas, aerosol, and CCN parameters, etc. The AWMDDB is situated approximately 5 km south of the entrance to the Huangshan Scenic Area. The presence

of tourists, especially a surge in tourists, has the potential to impact the atmospheric composition over the observation sites.

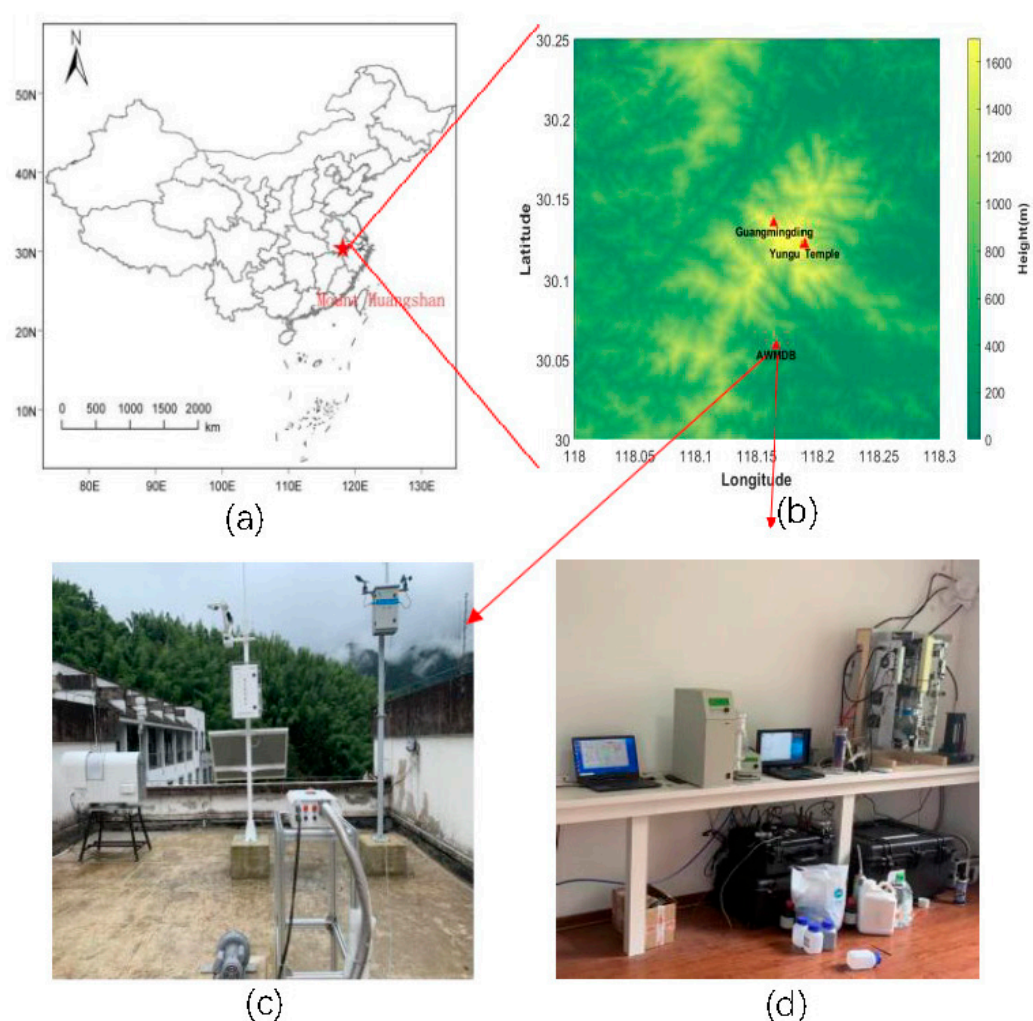


**Figure 1.** The locations of the field experiments and the instruments used: (a) Huangshan is shown by a red star and is located in the eastern region of China. (b) There are three observation points in the field campaign of the weather modification experiment in central China, the bottom of which is the research position of this paper. (c) Principal outdoor equipment at the AWMD. (d) Principal indoor instruments in the AWMD.

## 2.2. Ice-Nucleating Particle Measurements

The quantification of ice-nucleating particles was performed using a static vacuum vapor diffusion cloud chamber following the methodology described in our previously published articles [42–46]. The experimental setup involved the collection of aerosol particles on a silicon substrate using a high-voltage electrostatic aerosol collector. The collector possessed a cumulative capacity of 10 L of surrounding air and functioned with an airflow rate of 2 L per minute. The samples were gathered at 12:00 in the local time zone, which corresponds to UTC +8. From 27 April to 5 May 2023, a total of nine occurrences were evaluated. Every sample was obtained from a 45 mm silicon substrate and subjected to analysis at temperatures of  $-17$ ,  $-20$ ,  $-23$ , and  $-26$  °C, along with relative humidity levels of 95%, 97%, 99%, and 101%.

## 2.3. Determination of Aerosol Number Concentrations

A Scanning Electrical Mobility Spectrometer (SEMS Model 2100, Brechtel Mfg. Inc. Hayward, CA, USA) and Grimm 11-D optical particle counter (Grimm PAerosol Technik

GmbH & Co. KG, Airing, Germany) were used to measure the size distributions and concentrations of aerosol particles simultaneously. The SEMS recorded the size distributions of particles ranging from 10 to 500 nm during a sample period of 72 s. The particles were rendered electrically neutral by employing a soft X-ray aerosol charger (Model 9002, BMI Inc., Beverly Hills, CA, USA) prior to their introduction into the DMA (Differential Mobility Analyzer). The sheath and sample flow rates were adjusted to 5 L/min and 1 L/min, respectively. The Grimm 11-D optical particle counter utilizes light scattering to count and measure particles within the size range of 0.25 to 32  $\mu\text{m}$  across 31 different size channels. Before collecting samples, the tube through which the air enters and the nozzle of the device used to collect the samples were thoroughly cleaned. Additionally, the background count of the laser diode was reduced as instructed by the manufacturer. The Grimm was operated with a flow rate of 1.2 L per minute. The aerosol number concentration, expressed in particles per cubic centimeter (particles/cm<sup>3</sup>), was determined by integrating the counts across all size channels that were measured. Prior to each measurement, the device underwent zero calibration using a HEPA filter. The uncertainty was determined to be 10% by multiple calibrations utilizing particle standards.

#### 2.4. Electron Microscopy

Electron microscopy is a technique used to examine objects at a very high resolution by using a beam of electrons instead of light. INP samples were gathered onto silicon substrates using a high-voltage electrostatic aerosol collector for subsequent examination of their content and shape. The chosen substrates were examined using a high-resolution scanning electron microscope (SEM, ZEISS GeminiSEM 300, Oberkochen, Germany) that was equipped with energy dispersive X-ray spectroscopy (EDX). The determination of particle size and shape was conducted based on the analysis of SEM images. The elemental composition was determined by analyzing the EDS spectra with a ZAF correction.

### 3. Results and Discussion

#### 3.1. Observation of Ice Nucleation

The observed INP concentration over the Labor Day holiday is summarized in Figure 2. Ice nucleation occurs at temperatures ranging from  $-26\text{ }^{\circ}\text{C}$  to  $-17\text{ }^{\circ}\text{C}$  and a relative humidity spectrum ranging from 95% to 101%. Within these parameters, the INP concentration displayed a broad range, spanning from 0.1 to 30.5 ( $\text{L}^{-1}$ ). Notably, as the temperature decreased (from  $-17\text{ }^{\circ}\text{C}$  to  $-26\text{ }^{\circ}\text{C}$ ) and relative humidity increased (from 95% to 101%), there was a clear and substantial escalation in the ice nucleation concentration, as indicated in Figure 2a–d. The average INP concentration, particularly under the conditions of  $-26\text{ }^{\circ}\text{C}$  and 101% relative humidity, was observed to be  $13.7\text{ L}^{-1}$ . This concentration was, remarkably, 137 times greater than the INP concentration under the conditions of  $-17\text{ }^{\circ}\text{C}$  and 95% relative humidity. Furthermore, it was noted that the concentration of ice nuclei collected on various days exhibited fluctuations over time, with the highest values observed around April 29. During this peak period, the INP concentration was approximately half an order of magnitude greater than the minimum INP concentration recorded. These fluctuations may be attributed to factors like variations in meteorological conditions (temperature, humidity), concentrations of precursor aerosols, changes in aerosol sources/types (e.g., transportation, catering, etc.), and shifts in the intensity of human activities. These factors encompass not only variations in environmental conditions but also shifts in human activities, which could introduce changes in aerosol concentrations, as well as other environmental variables [4]. Thus, the observed fluctuations likely result from the complex interplay of these diverse influences on ice nucleation processes during the target period.

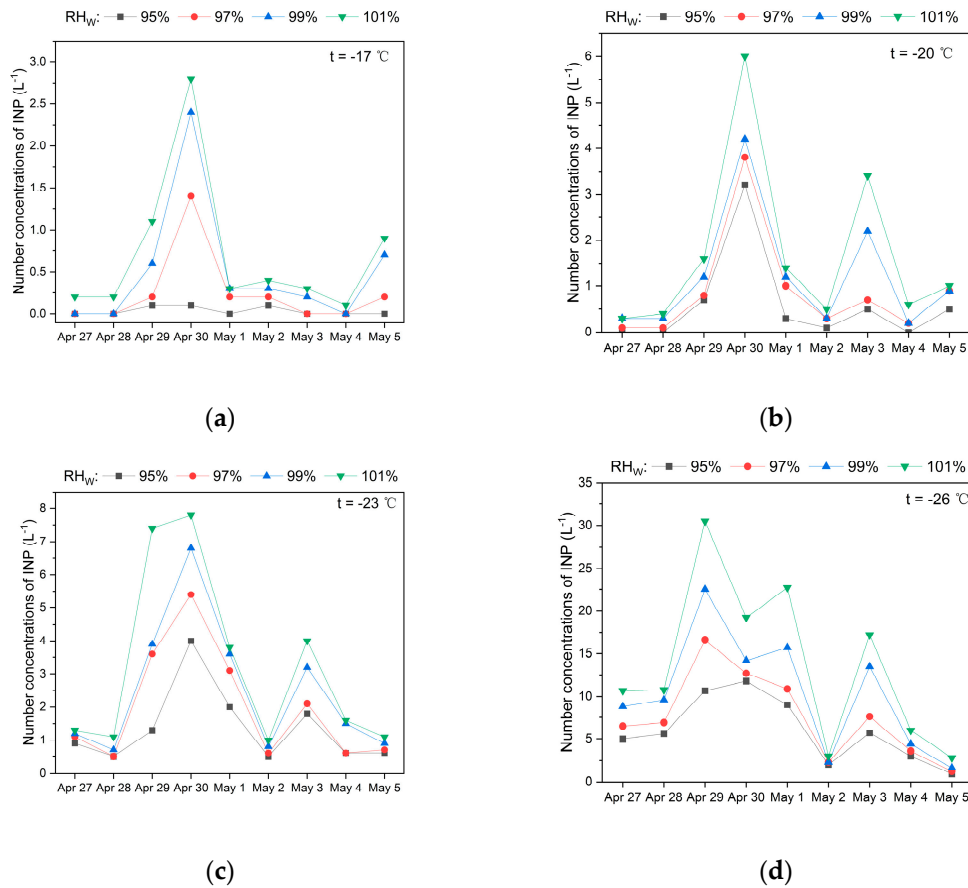


**Figure 2.** Time series of INP concentrations measured in Huangshan during the period from 27 April to 5 May 2023. (a)  $t = -17\text{ }^{\circ}\text{C}$ , RH<sub>w</sub> [95, 97, 99, 101]%, (b)  $t = -20\text{ }^{\circ}\text{C}$ , RH<sub>w</sub> [95, 97, 99, 101]%, (c)  $t = -23\text{ }^{\circ}\text{C}$ , RH<sub>w</sub> [95, 97, 99, 101]%, (d)  $t = -26\text{ }^{\circ}\text{C}$ , RH<sub>w</sub> [95, 97, 99, 101]%

The activation of ice-nucleating particles is predominantly influenced by temperature and humidity levels. Figure 3 illustrates the variations in INP concentrations at various levels of humidity and temperature. As anticipated based on prior observations [43,47], the concentrations of INPs escalates concomitantly with the decline in temperature and the elevation of relative humidity.

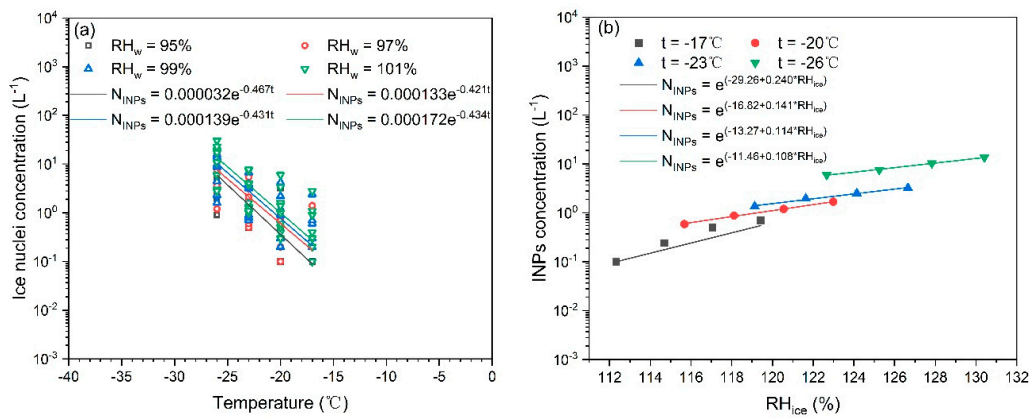


**Figure 3.** Number concentrations of INPs at different temperatures and different ice supersaturations in Huangshan, China. (a) All of the data on INP concentrations as a function of operating temperature; (b) the average INP concentrations under different ice supersaturation conditions.



Figure 3a shows the number concentration of INPs at various temperatures under different relative humidities. Several scholars have proposed that the number concentration of INPs can be parameterized based on the temperature [42,43]. The relationship between the concentration of INPs and the activation temperature is clearly exponential and can be fitted with the following equations:

$$N_{\text{INPs}} = 0.000032e^{-0.467t} (\text{RH}_w = 95\%) \quad (1)$$

$$N_{\text{INPs}} = 0.000133e^{-0.421t} (\text{RH}_w = 97\%) \quad (2)$$

$$N_{\text{INPs}} = 0.000139e^{-0.431t} (\text{RH}_w = 99\%) \quad (3)$$

$$N_{\text{INPs}} = 0.000172e^{-0.434t} (\text{RH}_w = 101\%) \quad (4)$$

where  $N_{\text{INPs}}$  is the concentration of INPs and  $t$  is the activation temperature.

Beyond temperature,  $\text{RH}_w$  stands as a pivotal factor influencing the concentration of INPs. Huffman demonstrated that relative humidity is an effective parameter for characterizing the deposition nucleation in observations of INPs [48]. Figure 3b illustrates the relationship between the average concentration of INPs and  $\text{RH}_w$  at specific temperatures. The data indicate that the concentration of INPs exhibited a substantial rise as the  $\text{RH}_w$  increased. In the past, researchers have used the following formula to calculate the relationship between INP concentrations and relative humidity [42,49]:

$$N_{\text{INPs}} = \exp(a + b \times \text{RH}_w) \quad (5)$$

Therefore, according to the data from this measurement, the optimal anticipated fit lines correspond to the following values:

$$N_{\text{INPs}} = e^{-29.26+0.240 \times \text{RH}_w} \quad t = -17 \text{ }^\circ\text{C} \quad (6)$$

$$N_{\text{INPs}} = e^{-16.82+0.141 \times \text{RH}_w} \quad t = -20 \text{ }^\circ\text{C} \quad (7)$$

$$N_{\text{INPs}} = e^{-13.27+0.114 \times \text{RH}_w} \quad t = -23 \text{ }^\circ\text{C} \quad (8)$$

$$N_{\text{INPs}} = e^{-11.46+0.108 \times \text{RH}_w} \quad t = -26 \text{ }^\circ\text{C} \quad (9)$$

Due to weaker activation of INPs at  $-17 \text{ }^\circ\text{C}$ , the squared correlation coefficients ( $R^2$ ) exhibit a lower value (0.5). At the other three temperatures, the  $R^2$  value exceeds 0.98. The primary factor is the diminished activation of ice nuclei at elevated temperatures ( $-17 \text{ }^\circ\text{C}$ ), particularly under conditions of low relative humidity, resulting in the absence of ice nuclei formation. Figure 4 presents the frequency distributions of INP concentrations at temperatures of  $-17 \text{ }^\circ\text{C}$ ,  $-20 \text{ }^\circ\text{C}$ ,  $-23 \text{ }^\circ\text{C}$ , and  $-26 \text{ }^\circ\text{C}$ . In Figure 4, samples that fall below the detection limit (or have zero active INPs) or, in a few cases, are overloaded, are not considered. Consequently, the distribution tails might be truncated since the extreme values are not sufficiently contained. The impact of this effect is anticipated to be more significant at a temperature of  $-17 \text{ }^\circ\text{C}$  due to a higher proportion of samples falling below the limit of detection at this temperature.

In Figure 3a,b, it is clear that a decrease of 1 degree in temperature leads to an increase in INP concentration, which closely resembles the effect of a three-unit increase in relative humidity. It appears that temperature fluctuations have a more significant impact on the concentration of ice-nucleating particles compared to changes in relative humidity. However, meteorologists generally concur that a 5% reduction in relative humidity results in an approximate 1 degree Celsius decline [50]. This suggests that the influence of relative humidity on the concentration of INPs is also extremely substantial.

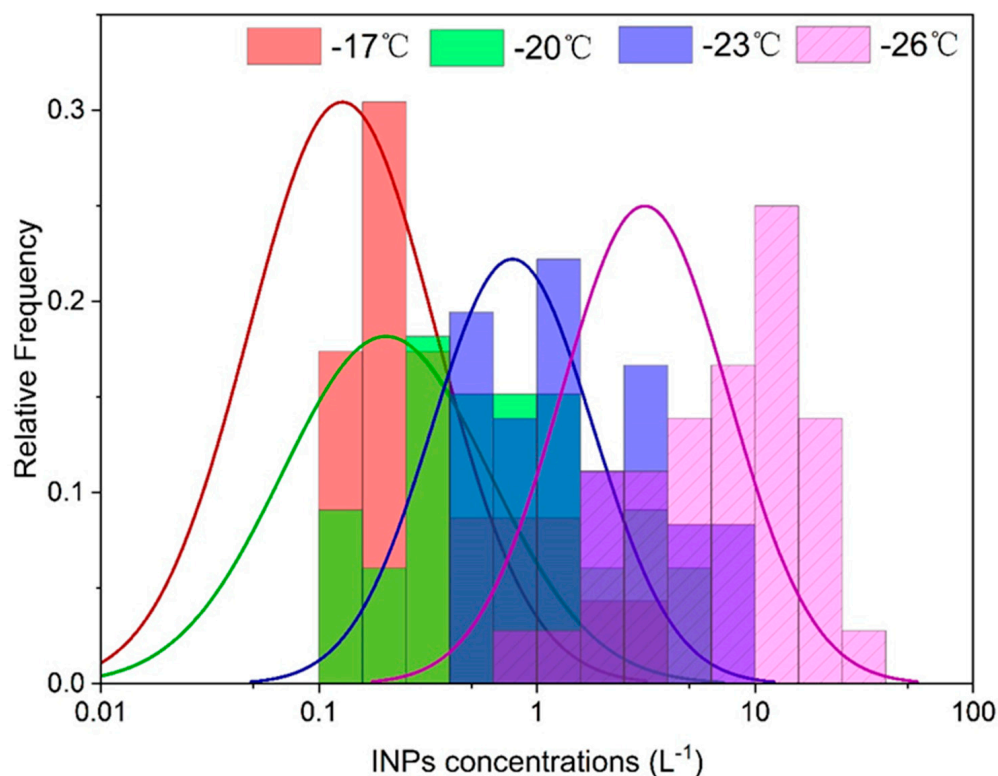


**Figure 4.** Probability density distribution plots of the INP concentrations at  $T = 17\text{ }^{\circ}\text{C}$ ,  $-20\text{ }^{\circ}\text{C}$ ,  $-23\text{ }^{\circ}\text{C}$ , and  $-26\text{ }^{\circ}\text{C}$ . The wavy colored lines represent the probability density normal fitting curves of different temperatures.

### 3.2. The Correlation between INP Concentration and Aerosol Size Distribution

While collecting INPs, the concentration of aerosol particles was measured simultaneously at the observation location. Figure 5 illustrates the time series of aerosol number concentrations in three distinct particle size ranges ( $0.01\text{ }\mu\text{m} < d < 0.5\text{ }\mu\text{m}$ ,  $d > 0.3\text{ }\mu\text{m}$ ,  $d > 0.5\text{ }\mu\text{m}$ ) throughout the observation period. As a result of human activities, it is evident that the concentration of aerosol particles larger than  $0.5\text{ }\mu\text{m}$  reaches its highest point on April 29, and there is another peak on 4 May. In the year 2023, China's labor holidays spanned from April 29th to May 3rd. The Huangshan Scenic Area, distinguished as a premier tourist destination in China, witnessed a surge in visitor influx commencing from the afternoon and evening of the day preceding the holiday. The departure of tourists persisted until the conclusion of the holiday period. Statistical analysis reveals a notable escalation in tourist numbers during the study period in 2023, totaling 117,835 visitors. This marks a remarkable increase of 399.62% compared to the preceding year, 2022 (<https://www.yixian.gov.cn/zwgk/public/6616535/11067195.html>, accessed on 21 May 2024).

The heightened anthropogenic activity accelerated the release of local aerosols, thereby influencing the quantity of INPs. The number concentration of INPs reached its highest point on April 29th and May 3rd, as shown in Figure 2. Previous studies have shown that the concentrations of activated INPs are correlated with concentrations of aerosols with diameters exceeding  $0.5\text{ }\mu\text{m}$  [42,44,51,52]. Therefore, the peak change in aerosols with a diameter greater than 0.5 microns is basically consistent with the peak of ice nucleation.

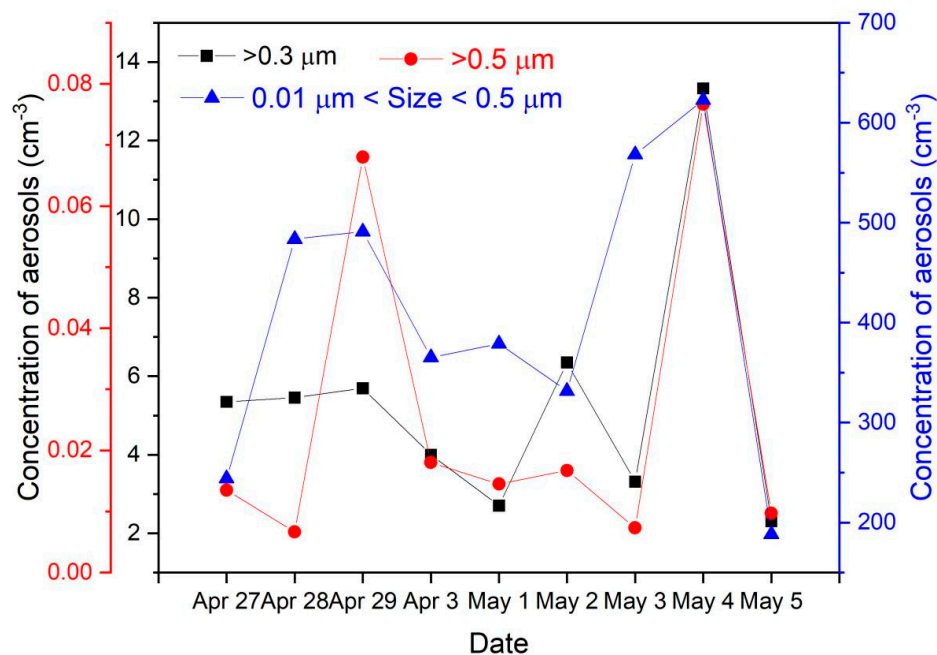


**Figure 5.** The fluctuations in the concentration of aerosol particles over the observation period.

### 3.3. Chemical Composition Characteristics of INPs: A Case

Multiple published studies have indicated that the activation rate of ice nuclei depends not only on the number concentration of aerosol, but also on its chemical composition. In this study, the morphological and chemical characteristics of the particles identified as INPs were analyzed using a SEM–EDX. We conducted measurements on INPs that exhibited activity at temperatures of  $-17$ ,  $-20$ ,  $-23$ , and  $-26$  °C, respectively. The EDX analysis was performed to semi-quantitatively analyze the presence of the elements N, O, Na, Mg, Al, S, Cl, K, Ca, Ti, and Cu in the particles. Overlapping Si peaks from the sampling substrate precluded Si in the analysis.

The findings of EDX analysis are depicted in Figure 6a. Due to the presence of oxygen in the atmosphere, the majority of elements in atmospheric particles undergo oxidation, making oxygen the predominant component. The concentrations of four elements (oxygen, nitrogen, chlorine, and sodium in certain ratios) were quantified for ice-nucleating particles that were activated at a temperature of  $-17$  °C. INPs possess a higher nitrogen content, which may be a mixture of biomass fragments (such as pollen, bacteria, seaweed, etc.) and sea salt. It has been explained that the particles might be more readily activated into INPs at higher temperatures. The INPs activated at temperatures of  $-20$  °C and  $-23$  °C were found to include five main elements: O, Na, Mg, Al, and K. Consequently, it is possible that the particles have aged like sea salt. INPs that were activated at a temperature of  $-26$  °C have successfully identified several elements with significant atomic sizes, such as O, Al, S, Cl, K, Ca, and Cu.

Aluminum and calcium are highly abundant metallic elements in Earth’s crust. Aluminum makes up around 7% of the crust’s mass, while calcium is found in diverse minerals such as limestone and gypsum [53]. These elements are frequently present in soil minerals and can be emitted into the atmosphere through natural processes like weathering, as well as human activities such as mining and construction [54,55]. Therefore, it is assumed that the aluminum and calcium found in air particulate matter come from sources related to Earth’s crust. In addition, the morphological features found in Figure 6e indicate that the particles have a greater diameter and a porous structure. Prior research has consistently found a direct relationship between the size of particles and the amount of aluminum they contain. Specifically, larger particles are likely to have higher concentrations of aluminum, as indicated by prior studies [56,57].



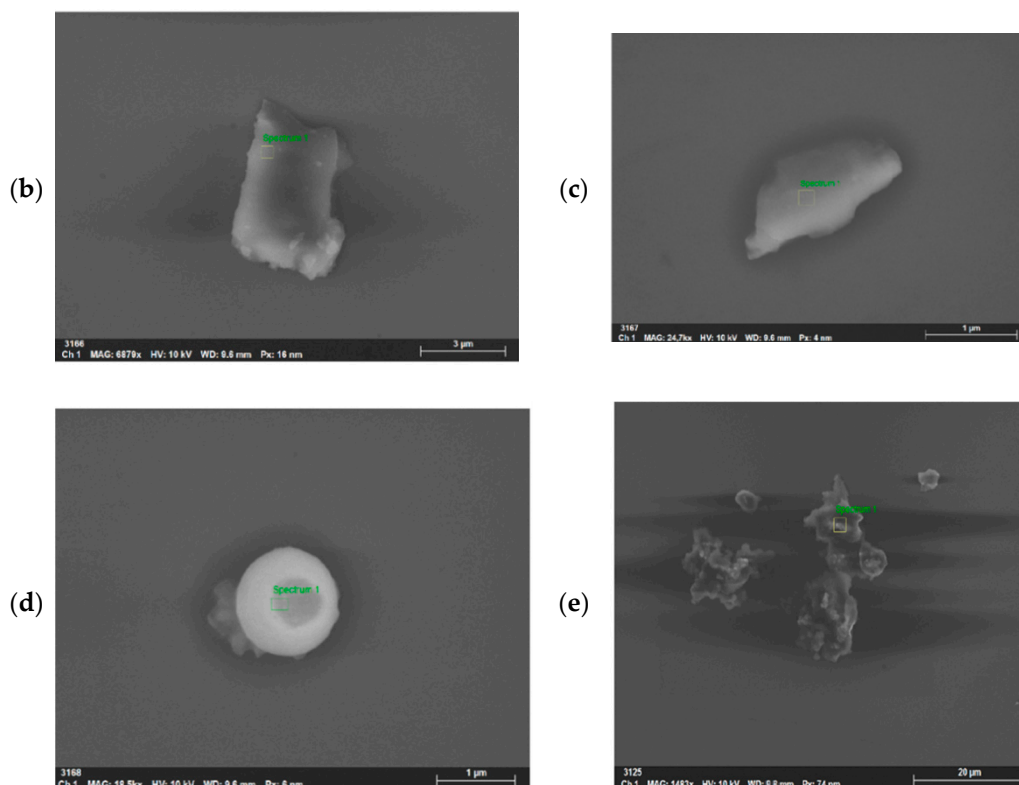
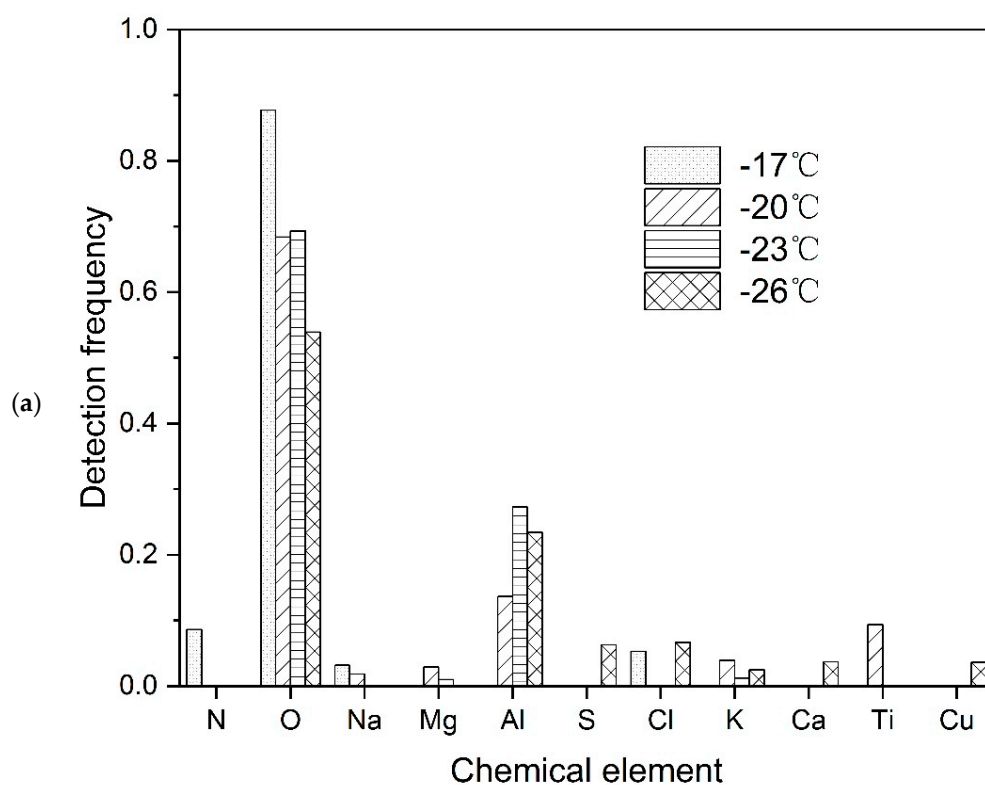


**Figure 6.** Summary of chemical and morphological characterization by scanning electron microscopy–energy-dispersive X-ray spectroscopy (SEM–EDX). The yellow box represents the area of SEM–EDX analysis. This green “Spectrum1” is the name of the first EDX spectrum collected. (a) Element proportion of INPs at different temperatures; (b) SEM image depicting the morphology of INPs at  $-17\text{ }^{\circ}\text{C}$ ; (c) SEM image illustrating the structure of INPs at  $-20\text{ }^{\circ}\text{C}$ ; (d) SEM image representing the shape of INPs at  $-23\text{ }^{\circ}\text{C}$ ; (e) SEM image showing the form of INPs at  $-26\text{ }^{\circ}\text{C}$ .

Prior research has thoroughly investigated the connection between the shape and composition of particles, as well as their possible origins, especially in relation to atmospheric aerosols [58,59]. The results of this study are consistent with the existing knowledge about mineral aerosols that originate from soil. These aerosols are distinguished by their bigger dimensions, irregular shapes, and porous architectures. They also contain components from Earth's crust, such as aluminum and calcium [53]. The observation, along with the permeable nature of the particles, substantiates the theory that this particulate matter may have its source in soil minerals. Based on the morphological characteristics found in Figure 6e, which shows particles with a greater diameter and a porous structure, it is possible that this particulate matter comes from soil minerals. Nevertheless, since this observation is based on a single instance, these attributions must be validated by more cases in order to be regarded as dependable evidence.

#### 4. Conclusions

This study performed comprehensive observation and research on INPs in Huangshan over the May Day holiday with the aim of acquiring a profound understanding of their physical and chemical characteristics. The concentration of INPs was quantified by collecting air samples using the newly built static vacuum water vapor diffusion chamber in Huangshan, located in the Anhui province of eastern China, over the period of 27 April to 5 May 2023. The concentrations of INPs were measured at activation temperatures of  $-17\text{ }^{\circ}\text{C}$ ,  $-20\text{ }^{\circ}\text{C}$ ,  $-23\text{ }^{\circ}\text{C}$ , and  $-25\text{ }^{\circ}\text{C}$ , together with relative humidity levels of 95%, 97%, 99%, and 101% relative to water. The primary findings and their consequences are presented below.

Similar to previous observations, successive reductions in temperature and elevations in relative humidity induced exponential escalations in measured INP concentrations. Under extreme conditions ( $-26\text{ }^{\circ}\text{C}$ , 101% RH), average levels attained  $13.7\text{ L}^{-1}$ , exceeding concentrations at  $-17\text{ }^{\circ}\text{C}$  and 95% RH by two orders of magnitude. Fluctuations in ice nucleation concentrations over time were observed, with notable concentration peaks around the beginning and end of labor holidays. The number concentration of INPs at various temperatures and relative humidity conditions is clearly exponential. The variables of temperature and relative humidity play a crucial role in the activation of ice nucleation. At a temperature of  $-17\text{ }^{\circ}\text{C}$ , the activation rate of INPs is low, resulting in a small R2 value for the parameterized equation of relative humidity and INPs. However, at three other temperatures ( $-20\text{ }^{\circ}\text{C}$ ,  $-23\text{ }^{\circ}\text{C}$ , and  $-26\text{ }^{\circ}\text{C}$ ), the R2 value for the parameterized equation of relative humidity and INPs exceeds 0.98.

Human activities have led to a rise in aerosol concentrations, which were seen to be high during the May Day holiday. The maximum variation in aerosols larger than 0.5 microns in diameter aligns with the highest point of ice nucleation. This is supported by prior research indicating that the level of activated INPs is linked to aerosols with sizes surpassing  $0.5\text{ }\mu\text{m}$ .

Furthermore, a crucial component of this investigation involves a comprehensive examination of the chemical makeup of INPs using SEM-EDX with the aim of uncovering their distinct elemental composition, which is contingent upon their activation temperature. The nitrogen, sodium, and chlorine observed in INPs activated at  $-17\text{ }^{\circ}\text{C}$  suggests the presence of biomass fragments and sea salt. Conversely, INPs activated at  $-20\text{ }^{\circ}\text{C}$  and  $-23\text{ }^{\circ}\text{C}$  exhibited five elements (O, Na, Mg, Al, and K), possibly the distinctive components of aged sea salt. It is important to mention that INPs activated at a temperature of  $-26\text{ }^{\circ}\text{C}$  exhibited elemental properties associated with Earth.

This study provides a comprehensive examination of atmospheric ice-nucleating particles in Huangshan during the Labor Day holiday. This study makes a substantial contribution to the field of atmospheric science by investigating the diverse effects of human activities on the properties of aerosols and the subsequent processes of ice nucleation. The application of comprehensive methodologies, such as INP measurements, aerosol size distribution analyses, and SEM-EDX investigations, enhances the scientific validity of the findings. However, it is important to note that the research duration was relatively

short, and the amount of data collected during this period may not be sufficient to draw definitive conclusions. Some of the findings and conclusions presented in this study would benefit from further observations and support from additional case studies conducted over longer periods and across different seasons or locations. Nonetheless, this study lays the foundation for future research aimed at gaining a deeper understanding of the complex interplay between anthropogenic activities, aerosol properties, and ice nucleation processes.

**Author Contributions:** Conceptualization, methodology, investigation, X.C, L.J., and S.Z.; data curation, software, X.C.; original draft preparation, K.C.; funding acquisition, supervision, project administration, Y.Y. All authors have read and agreed to the published version of the manuscript.

**Funding:** This study was supported by the Central Region Artificial Weather Influence Capacity Building Project Huangshan Cloud and Fog Observation Experiment (ZQC-T22253); Nanjing University of Information Science and Technology Party Construction Research Project (2023nxddj-bc33).

**Institutional Review Board Statement:** Not applicable.

**Informed Consent Statement:** Not applicable.

**Data Availability Statement:** The datasets generated and analyzed during the current study are available from the corresponding author upon reasonable request. The data are not publicly available due to ongoing longitudinal analysis.

**Acknowledgments:** The authors are grateful to the editors and anonymous reviewers for their insightful comments and helpful suggestions.

**Conflicts of Interest:** The authors declare no conflict of interest.

## References

1. Zauscher, M.D.; Moore, M.J.K.; Lewis, G.S.; Hering, S.V.; Prather, K.A. Approach for Measuring the Chemistry of Individual Particles in the Size Range Critical for Cloud Formation. *Anal. Chem.* **2011**, *83*, 2271–2278. [[CrossRef](#)] [[PubMed](#)]
2. Lenaerts, J.T.M.; Van Tricht, K.; Lhermitte, S.; L'Ecuyer, T.S. Polar clouds and radiation in satellite observations, reanalyses, and climate models. *Geophys. Res. Lett.* **2017**, *44*, 3355–3364. [[CrossRef](#)]
3. Sanghavi, S.; Lebsock, M.; Stephens, G. Sensitivity analysis of polarimetric O<sub>2</sub> A-band spectra for potential cloud retrievals using OCO-2/GOSAT measurements. *Atmos. Meas. Tech.* **2015**, *8*, 3601–3616. [[CrossRef](#)]
4. Schrod, J.; Thomson, E.S.; Weber, D.; Kossmann, J.; Pöhlker, C.; Saturno, J.; Ditas, F.; Artaxo, P.; Clouard, V.; Saurel, J.-M. Long-term deposition and condensation ice-nucleating particle measurements from four stations across the globe. *Atmos. Chem. Phys.* **2020**, *20*, 15983–16006. [[CrossRef](#)]
5. Zhao, X.; Liu, X.; Burrows, S.M.; Shi, Y. Effects of marine organic aerosols as sources of immersion-mode ice-nucleating particles on high-latitude mixed-phase clouds. *Atmos. Chem. Phys.* **2021**, *21*, 2305–2327. [[CrossRef](#)]
6. Bellouin, N.; Quaas, J.; Gryspeerdt, E.; Kinne, S.; Stier, P.; Watson-Parris, D.; Boucher, O.; Carslaw, K.S.; Christensen, M.; Daniau, A.L. Bounding global aerosol radiative forcing of climate change. *Rev. Geophys.* **2020**, *58*, e2019RG000660. [[CrossRef](#)] [[PubMed](#)]
7. Liu, M.; Matsui, H. Aerosol radiative forcings induced by substantial changes in anthropogenic emissions in China from 2008 to 2016. *Atmos. Chem. Phys.* **2021**, *21*, 5965–5982. [[CrossRef](#)]
8. DeMott, P.J.; Prenni, A.J.; Liu, X.; Kreidenweis, S.M.; Petters, M.D.; Twohy, C.H.; Richardson, M.; Eidhammer, T.; Rogers, D. Predicting global atmospheric ice nuclei distributions and their impacts on climate. *Proc. Natl. Acad. Sci. USA* **2010**, *107*, 11217–11222. [[CrossRef](#)] [[PubMed](#)]
9. Alizadeh-Choobari, O.; Gharaylou, M. Aerosol impacts on radiative and microphysical properties of clouds and precipitation formation. *Atmos. Res.* **2017**, *185*, 53–64. [[CrossRef](#)]
10. Gettelman, A.; Liu, X.; Barahona, D.; Lohmann, U.; Chen, C. Climate impacts of ice nucleation. *J. Geophys. Res. Atmos.* **2012**, *117*, D20. [[CrossRef](#)]
11. DeMott, P.J.; Mason, R.H.; McCluskey, C.S.; Hill, T.C.; Perkins, R.J.; Desyaterik, Y.; Bertram, A.K.; Trueblood, J.V.; Grassian, V.H.; Qiu, Y. Ice nucleation by particles containing long-chain fatty acids of relevance to freezing by sea spray aerosols. *Environ. Sci. Process. Impacts* **2018**, *20*, 1559–1569. [[CrossRef](#)] [[PubMed](#)]
12. Marcolli, C.; Nagare, B.; Welts, A.; Lohmann, U. Ice nucleation efficiency of AgI: Review and new insights. *Atmos. Chem. Phys.* **2016**, *16*, 8915–8937. [[CrossRef](#)]
13. Liu, X. Heterogeneous nucleation or homogeneous nucleation? *J. Chem. Phys.* **2000**, *112*, 9949–9955. [[CrossRef](#)]
14. Madras, G.; McCoy, B.J. Temperature effects on the transition from nucleation and growth to Ostwald ripening. *Chem. Eng. Sci.* **2004**, *59*, 2753–2765. [[CrossRef](#)]
15. Simpson, E.L.; Connolly, P.J.; McFiggans, G. Competition for water vapour results in suppression of ice formation in mixed-phase clouds. *Atmos. Chem. Phys.* **2018**, *18*, 7237–7250. [[CrossRef](#)]

16. Zhang, M.; Liu, X.; Diao, M.; D'Alessandro, J.J.; Wang, Y.; Wu, C.; Zhang, D.; Wang, Z.; Xie, S. Impacts of representing heterogeneous distribution of cloud liquid and ice on phase partitioning of Arctic mixed-phase clouds with NCAR CAM5. *J. Geophys. Res. Atmos.* **2019**, *124*, 13071–13090. [[CrossRef](#)]
17. Tao, W.K.; Chen, J.P.; Li, Z.; Wang, C.; Zhang, C. Impact of aerosols on convective clouds and precipitation. *Rev. Geophys.* **2012**, *50*, 2. [[CrossRef](#)]
18. Burrows, S.M.; McCluskey, C.S.; Cornwell, G.; Steinke, I.; Zhang, K.; Zhao, B.; Zawadowicz, M.; Raman, A.; Kulkarni, G.; China, S. Ice-nucleating particles that impact clouds and climate: Observational and modeling research needs. *Rev. Geophys.* **2022**, *60*, e2021RG000745. [[CrossRef](#)]
19. Rangel-Alvarado, R.; Li, H.; Ariya, P.A. Snow particles physiochemistry: Feedback on air quality, climate change, and human health. *Environ. Sci. Atmos.* **2022**, *2*, 891–920. [[CrossRef](#)]
20. Riemer, N.; Ault, A.; West, M.; Craig, R.; Curtis, J. Aerosol mixing state: Measurements, modeling, and impacts. *Rev. Geophys.* **2019**, *57*, 187–249. [[CrossRef](#)]
21. Lacher, L.; Steinbacher, M.; Bukowiecki, N.; Herrmann, E.; Zipori, A.; Kanji, Z.A. Impact of air mass conditions and aerosol properties on ice nucleating particle concentrations at the High Altitude Research Station Jungfraujoch. *Atmosphere* **2018**, *9*, 363. [[CrossRef](#)]
22. Huang, S.; Hu, W.; Chen, J.; Wu, Z.; Zhang, D.; Fu, P. Overview of biological ice nucleating particles in the atmosphere. *Environ. Int.* **2021**, *146*, 106197. [[CrossRef](#)] [[PubMed](#)]
23. Sekiguchi, M.; Nakajima, T.; Suzuki, K.; Kawamoto, K.; Higurashi, A.; Rosenfeld, D.; Sano, I.; Mukai, S. A study of the direct and indirect effects of aerosols using global satellite data sets of aerosol and cloud parameters. *J. Geophys. Res. Atmos.* **2003**, *108*, D22. [[CrossRef](#)]
24. McComiskey, A.; Feingold, G. The scale problem in quantifying aerosol indirect effects. *Atmos. Chem. Phys.* **2012**, *12*, 1031–1049. [[CrossRef](#)]
25. Gryspeerdt, E.; Quaas, J.; Bellouin, N. Constraining the aerosol influence on cloud fraction. *J. Geophys. Res. Atmos.* **2016**, *121*, 3566–3583. [[CrossRef](#)]
26. Cornwell, G.C.; McCluskey, C.S.; Hill, T.C.; Levin, E.T.; Rothfuss, N.E.; Tai, S.-L.; Petters, M.D.; DeMott, P.J.; Kreidenweis, S.; Prather, K.A. Bioaerosols are the dominant source of warm-temperature immersion-mode INPs and drive uncertainties in INP predictability. *Sci. Adv.* **2023**, *9*, eadg3715. [[CrossRef](#)] [[PubMed](#)]
27. Murray, B.; O'sullivan, D.; Atkinson, J.; Webb, M. Ice nucleation by particles immersed in supercooled cloud droplets. *Chem. Soc. Rev.* **2012**, *41*, 6519–6554. [[CrossRef](#)] [[PubMed](#)]
28. Hoose, C.; Möhler, O. Heterogeneous ice nucleation on atmospheric aerosols: A review of results from laboratory experiments. *Atmos. Chem. Phys.* **2012**, *12*, 9817–9854. [[CrossRef](#)]
29. Morris, C.E.; Georgakopoulos, D.G.; Sands, D.C. Ice nucleation active bacteria and their potential role in precipitation. *J. De Phys. IV Proc.* **2004**, *121*, 87–103. [[CrossRef](#)]
30. Connolly, P.; Möhler, O.; Field, P.; Saathoff, H.; Burgess, R.; Choularton, T.; Gallagher, M. Studies of heterogeneous freezing by three different desert dust samples. *Atmos. Chem. Phys.* **2009**, *9*, 2805–2824. [[CrossRef](#)]
31. Niemand, M. A Particle-Surface-Area-Based Formulation of Heterogeneous Ice Nucleation by Mineral Dust Aerosols. Ph.D. Thesis, Karlsruhe, Karlsruher Institut für Technologie (KIT), Karlsruhe, Germany, 2012.
32. Koehler, K.A.; DeMott, P.J.; Kreidenweis, S.M.; Popovicheva, O.B.; Petters, M.D.; Carrico, C.M.; Kireeva, E.D.; Khokhlova, T.D.; Shonija, N.K. Cloud condensation nuclei and ice nucleation activity of hydrophobic and hydrophilic soot particles. *Phys. Chem. Chem. Phys.* **2009**, *11*, 7906–7920. [[CrossRef](#)]
33. DeMott, P.J. An exploratory study of ice nucleation by soot aerosols. *J. Appl. Meteorol. Climatol.* **1990**, *29*, 1072–1079. [[CrossRef](#)]
34. Santachiara, G.; Prodi, F.; Belosi, F.; Nicosia, A. A Review of Thermo-and Diffusio-Phoresis in the Atmospheric Aerosol Scavenging Process. Part 2: Ice Crystal and Snow Scavenging. *Atmos. Clim. Sci.* **2023**, *13*, 466–477. [[CrossRef](#)]
35. Eriksen Hammer, S.; Mertes, S.; Schneider, J.; Ebert, M.; Kandler, K.; Weinbruch, S. Composition of ice particle residuals in mixed-phase clouds at Jungfraujoch (Switzerland): Enrichment and depletion of particle groups relative to total aerosol. *Atmos. Chem. Phys.* **2018**, *18*, 13987–14003. [[CrossRef](#)]
36. Calvo, A.; Alves, C.; Castro, A.; Pont, V.; Vicente, A.; Fraile, R. Research on aerosol sources and chemical composition: Past, current and emerging issues. *Atmos. Res.* **2013**, *120*, 1–28. [[CrossRef](#)]
37. Usher, C.R.; Michel, A.E.; Grassian, V.H. Reactions on mineral dust. *Chem. Rev.* **2003**, *103*, 4883–4940. [[CrossRef](#)] [[PubMed](#)]
38. Augustin-Bauditz, S.; Wex, H.; Denjean, C.; Hartmann, S.; Schneider, J.; Schmidt, S.; Ebert, M.; Stratmann, F. Laboratory-generated mixtures of mineral dust particles with biological substances: Characterization of the particle mixing state and immersion freezing behavior. *Atmos. Chem. Phys.* **2016**, *16*, 5531–5543. [[CrossRef](#)]
39. Kulkarni, G.; Sanders, C.; Zhang, K.; Liu, X.; Zhao, C. Ice nucleation of bare and sulfuric acid-coated mineral dust particles and implication for cloud properties. *J. Geophys. Res. Atmos.* **2014**, *119*, 9993–10011. [[CrossRef](#)]
40. Sullivan, R.; Petters, M.D.; DeMott, P.J.; Kreidenweis, S.M.; Wex, H.; Niedermeier, D.; Hartmann, S.; Clauss, T.; Stratmann, F.; Reitz, P. Irreversible loss of ice nucleation active sites in mineral dust particles caused by sulphuric acid condensation. *Atmos. Chem. Phys.* **2010**, *10*, 11471–11487. [[CrossRef](#)]

41. Che, Y.; Zhang, J.; Zhao, C.; Fang, W.; Xue, W.; Yang, W.; Ji, D.; Dang, J.; Duan, J.; Sun, J. A study on the characteristics of ice nucleating particles concentration and aerosols and their relationship in spring in Beijing. *Atmos. Res.* **2021**, *247*, 105196. [[CrossRef](#)]
42. Chen, K.; Yin, Y.; Liu, S.; Liu, C.; Wang, H.; He, C.; Jiang, H.; Chen, J. Concentration and variability of deposition-mode ice nucleating particles from Mt. Tai China in the Early Summer. *Atmos. Res.* **2021**, *253*, 105426. [[CrossRef](#)]
43. Jiang, H.; Yin, Y.; Chen, K.; Chen, Q.; He, C.; Sun, L. The measurement of ice nucleating particles at Tai'an city in East China. *Atmos. Res.* **2020**, *232*, 104684. [[CrossRef](#)]
44. Jiang, H.; Yin, Y.; Wang, X.; Gao, R.; Yuan, L.; Chen, K.; Shan, Y. The measurement and parameterization of ice nucleating particles in different backgrounds of China. *Atmos. Res.* **2016**, *181*, 72–80. [[CrossRef](#)]
45. Steinke, I.; Hoose, C.; Möhler, O.; Connolly, P.; Leisner, T. A new temperature- and humidity-dependent surface site density approach for deposition ice nucleation. *Atmos. Chem. Phys.* **2015**, *15*, 3703–3717. [[CrossRef](#)]
46. Shen, L.-J.; Wang, H.-L.; Yin, Y.; Chen, K.; Chen, J.-H.; Shi, S.-S. Size Distributions of Aerosol During the Summer at the Summit of Mountain Taishan (1534 m) in Central East China. *Huan Jing Ke Xue = Huanjing Kexue* **2019**, *40*, 2019–2026. [[PubMed](#)]
47. Wu, J.; Yin, Y.; Chen, K.; He, C.; Jiang, H.; Zheng, B.; Li, B.; Li, Y.; Lv, Y. Vertical Distribution of Atmospheric Ice Nucleating Particles in Winter over Northwest China Based on Aircraft Observations. *Atmosphere* **2022**, *13*, 1447. [[CrossRef](#)]
48. Huffman, P.J. Supersaturation Spectra of AgI and Natural Ice Nuclei. *J. Appl. Meteorol. (1962–1982)* **1973**, *12*, 1080–1082. [[CrossRef](#)]
49. Meyers, M.; DeMott, P.; Cotton, W. New Primary Ice-Nucleation Parameterizations in an Explicit Cloud Model. *J. Appl. Meteorol. Climatol.* **1982**, *31*, 708–721. [[CrossRef](#)]
50. Lawrence, M.G. The Relationship between Relative Humidity and the Dewpoint Temperature in Moist Air: A Simple Conversion and Applications. *Bull. Am. Meteorol. Soc.* **2005**, *86*, 225–233. [[CrossRef](#)]
51. DeMott, P.J.; Möhler, O.; Stetzer, O.; Vali, G.; Levin, Z.; Petters, M.D.; Murakami, M.; Leisner, T.; Bundke, U.; Klein, H. Resurgence in ice nuclei measurement research. *Bull. Am. Meteorol. Soc.* **2011**, *92*, 1623–1635. [[CrossRef](#)]
52. Mason, R.; Si, M.; Chou, C.; Irish, V.; Dickie, R.; Elizondo, P.; Wong, R.; Brintnell, M.; Elsasser, M.; Lassar, W. Size-resolved measurements of ice-nucleating particles at six locations in North America and one in Europe. *Atmos. Chem. Phys.* **2016**, *16*, 1637–1651. [[CrossRef](#)]
53. Rauch, J.N.; Pacyna, J.M. Earth's global Ag, Al, Cr, Cu, Fe, Ni, Pb, and Zn cycles. *Glob. Biogeochem. Cycle* **2009**, *23*, 16. [[CrossRef](#)]
54. Zhang, Q.; Wang, C. Natural and human factors affect the distribution of soil heavy metal pollution: A review. *Water Air Soil Pollut.* **2020**, *231*, 350. [[CrossRef](#)]
55. Nortjé, G.P.; Laker, M.C. Factors that determine the sorption of mineral elements in soils and their impact on soil and water pollution. *Minerals* **2021**, *11*, 821. [[CrossRef](#)]
56. Blocken, B.; Van Druenen, T.; Ricci, A.; Kang, L.; Van Hooff, T.; Qin, P.; Xia, L.; Ruiz, C.A.; Arts, J.; Diepens, J. Ventilation and air cleaning to limit aerosol particle concentrations in a gym during the COVID-19 pandemic. *Build. Environ.* **2021**, *193*, 107659. [[CrossRef](#)]
57. Wang, J.; Li, J.; Liu, S.; Li, H.; Chen, X.; Peng, C.; Zhang, P.; Liu, X. Distinct microplastic distributions in soils of different land-use types: A case study of Chinese farmlands. *Environ. Pollut.* **2021**, *269*, 116199. [[CrossRef](#)]
58. Shao, L.; Liu, P.; Jones, T.; Yang, S.; Wang, W.; Zhang, D.; Li, Y.; Yang, C.-X.; Xing, J.; Hou, C. A review of atmospheric individual particle analyses: Methodologies and applications in environmental research. *Gondwana Res.* **2022**, *110*, 347–369. [[CrossRef](#)]
59. Murphy, D.M.; Froyd, K.D.; Bourgeois, I.; Brock, C.A.; Kupc, A.; Peischl, J.; Schill, G.P.; Thompson, C.R.; Williamson, C.J.; Yu, P. Radiative and chemical implications of the size and composition of aerosol particles in the existing or modified global stratosphere. *Atmos. Chem. Phys.* **2021**, *21*, 8915–8932. [[CrossRef](#)]

**Disclaimer/Publisher's Note:** The statements, opinions and data contained in all publications are solely those of the individual author(s) and contributor(s) and not of MDPI and/or the editor(s). MDPI and/or the editor(s) disclaim responsibility for any injury to people or property resulting from any ideas, methods, instructions or products referred to in the content.